Chemistry of [Ru(1,3-diaryltriazenide)$_2$(PPh$_3$)$_2$]^z (z = 0, +). A Hindered Ru^{II,III}N$_4$P$_2$ Family with Valence-Independent Geometry

Mahua Menon, Amitava Pramanik, Surajit Chattopadhyay, Nilkamal Bag, and Animesh Chakravorty*

Department of Inorganic Chemistry, Indian Association for the Cultivation of Science, Calcutta 700 032, India

Received August 29, 1994[⊗]

The reaction of Ru(PPh$_3$)$_3$Cl$_2$ with 1,3-diaryltriazenes, (p-RC$_6$H$_4$N)(p-RC$_6$H$_4$NH)N (HRL; R = H, Me, OMe, Cl), in ethanol affords Ru^{II}(RL)$_2$(PPh$_3$)$_2$, which is oxidized by cerium(IV) to the trivalent complex isolated as [Ru^{III}(RL)$_2$(PPh$_3$)$_2$]PF$_6$. Yields are near-quantitative for both oxidation states. The X-ray structures of Ru(HL)$_2$(PPh$_3$)$_2$ and [Ru(ClL)$_2$(PPh$_3$)$_2$]PF$_6$·2CH$_2$Cl$_2$ have revealed centrosymmetric trans geometry for both RuN$_4$P$_2$ coordination spheres. The four-membered triazenide chelate rings are near-perfect planes, and the average Ru−N length decreases by ~0.04 Å in going from the bivalent to the trivalent complex due to the contraction of the metal radius in the primarily σ-bonded RuN$_4$ frame. In contrast, the Ru−P length is ~0.07 Å shorter in the bivalent complex because of strong Ru−P 4dπ−3dπ back-bonding, which is lacking in the trivalent complex. Studies on the energetics of models have revealed that cis geometry is precluded by severe steric crowding of triazenide vis-à-vis phosphine aryl functions. The repulsions are very strong even in the "best" rotameric configurations of triazene aryls. The bivalent complexes are diamagnetic and display an MLCT band near 500 nm. The trivalent species have one unpaired electron (1.78−1.86 μ_B), and they show a strong band near 1200 nm which has been assigned to LMCT excitation ($a_u \rightarrow a_g$, b_g) on the basis of model EHMO results. The $E_{1/2}$ values of the stereoretentive ruthenium(III)−ruthenium(II) couple lie in the range 0.08−0.37 V vs SCE, increasing in the order OMe < Me < H < Cl. Crystal data for the complexes are as follows: Ru(HL)$_2$(PPh$_3$)$_2$, crystal system triclinic, space group $P\bar{1}$; a = 10.964(6) Å, b = 11.821(7) Å, c = 21.183(9) Å, α = 76.52(4)°, β = 78.17(4)°, γ = 71.18(4)°, V = 2502(2) Å^3, Z = 2, R = 3.93%, R_w = 4.32%; [Ru(ClL)$_2$(PPh$_3$)$_2$]PF$_6$·2CH$_2$Cl$_2$, crystal system triclinic; space group $P\bar{1}$, a = 11.093(6) Å, b = 12.386(4) Å, c = 13.757(6) Å, α = 104.11(3)°, β = 103.48(4)°, γ = 110.57(3)°, V = 1607(1) Å^3, Z = 1, R = 5.00%, R_w = 5.64%.

Introduction

The differentiation of isomeric coordination spheres by transition metal oxidation states is an important facet of variable-valence chemistry.[1−3] We recently showed that ruthenium and osmium systems of the type [M(XCS$_2$)$_2$(PPh$_3$)$_2$]^z (X = OR, SR, NR$_2$) display strong valence-geometry selectivity, the preferred combinations being bivalent-cis (z = 0) and trivalent-trans (z = +). Available evidence suggests that the seat of differentiation is the M(PPh$_3$)$_2$ fragment and the instruments of differentiation are M−P back-bonding and phosphine crowding.[4−6]

In the present study, the link between ruthenium valence and geometry is scrutinized in a new situation. Herein we describe the design, structure, and properties of a family of complexes in which the Ru(PPh$_3$)$_2$ motif is still present but the differentiation phenomenon is muted by interference from outside the motif. The result is valence independence of geometrical structure.

* Telefax: +91-33-473-2805. Email: icac@iacs.ernet.in.

[⊗] Abstract published in *Advance ACS Abstracts,* February 1, 1995.

(1) (a) Pramanik, A.; Bag, N.; Chakravorty, A. *Inorg. Chem.* **1993**, *32*, 811. (b) Basu, P.; Chakravorty, A. *Inorg. Chem.* **1992**, *31*, 4980 and references therein. (c) Basu, P.; Bhanja Choudhury, S.; Pal, S.; Chakravorty, A. *Inorg. Chem.* **1989**, *28*, 2680.

(2) (a) Bond, A. M.; Colton, R.; Kevekordes, J. E.; Panagioditon, P. *Inorg. Chem.* **1987**, *26*, 1430. (b) Bond, A. M.; Hambley, T. W.; Mann, D. R.; Snow, M. R. *Inorg. Chem.* **1987**, *26*, 2257 and references therein.

(3) (a) Evans, D. H.; O'Connell, K. M. In *Electroanalytical Chemistry. A Series of Advances*; Bard, A. J., Ed.; Marcel Dekker: New York, 1986; Vol. 14, p 113. (b) Geiger, W. E. *Prog. Inorg. Chem.* **1985**, *33*, 275.

(4) X = OR: (a) Pramanik, A.; Bag, N.; Ray, D.; Lahiri, G. K.; Chakravorty, A. *Inorg. Chem.* **1991**, *30*, 410. (b) Bag, N.; Lahiri, G. K.; Chakravorty, A. *J. Chem. Soc., Dalton Trans.* **1990**, 1557.

Results and Discussion

A. System Choice and Synthesis. In search of systems of type Ru(bidentate)$_2$(PPh$_3$)$_2^z$ where the bidentate ligand may also be actively involved in the control of isomer stability, we have examined 1,3-diaryltriazenes (general abbreviation HRL) as bidentate ligands. A comparison of the four-membered chelate binding in Ru(RL) with that in Ru(XCS$_2$) would be interesting, but the more important objective of this choice is to assess the possible effect of the pendant aryl groups of Ru(RL) on isomer preference.

Four triazene ligands (R = H, Me, OMe, Cl) have been utilized in the present work. The red diamagnetic bivalent complexes Ru(RL)$_2$(PPh$_3$)$_2$, **1**, were obtained in nearly quantitative yields from the stoichiometric reaction of eq 1 carried out in

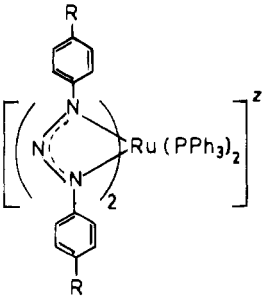

R = H, Me, OMe, Cl

1 z = 0

2 z = +

0020-1669/95/1334-1361$09.00/0

$$Ru(PPh_3)_3Cl_2 + 2HRL \rightarrow Ru(RL)_2(PPh_3)_2 + 2HCl \quad (1)$$

boiling ethanol. In earlier syntheses $RuH_2(PPh_3)_4$ and $RuCl_2(PPh_3)_4$ have been used but yields were not as good.[7a-c]

The brownish-red trivalent complexes $[Ru(RL)_2(PPh_3)_2]PF_6$ are reported here for the first time. These were obtained by oxidizing solutions of **1** in dichloromethane–acetonitrile by aqueous cerium(IV), eq 2. Single crystals of the ClL^- complex

$$Ru(RL)_2(PPh_3)_2 + Ce(IV) + PF_6^- \rightarrow [Ru(RL)_2(PPh_3)_2]PF_6 + Ce(III) \quad (2)$$

grown from dichloromethane–hexane contain dichloromethane of crystallization (see below). The salts act as one-electron paramagnets (d^5) and in acetonitrile solution behave as 1:1 electrolytes (Table 1).

B. Structure. The X-ray structures of $Ru^{II}(HL)_2(PPh_3)_2$ and $[Ru^{III}(ClL)_2(PPh_3)_2]PF_6 \cdot 2CH_2Cl_2$ have been determined. Only one[7d] mononuclear Ru(RL) structure is known.[8] Perspective views and atom-labeling schemes are shown in Figures 1 and 2, and selected bond parameters are listed in Tables 2 and 3. Both complexes belong to the space group $P\bar{1}$, and in both the metal atoms lie at special positions implying molecular centrosymmetry and hence trans geometry. In the bivalent complex two independent positions (0, 0, 0 and 0, $^1/_2$, $^1/_2$) are occupied; the two crystallographically distinct molecules are however metrically very similar. In the trivalent complex (Ru at 0, 0, 0) the PF_6^- anion is also centrosymmetric (P at 0, 0, $^1/_2$); the dichloromethane molecules lie in general positions.

In both complexes, the triazenide ligands bind in the four-membered chelate mode with bite angles near 60°. The angular distortions of the RuN_4P_2 coordination spheres from ideal octahedral geometry are thus severe. The P–Ru–P axis is nearly but not exactly perpendicular to the plane of the chelate rings in either case. The point group symmetry of the coordination spheres of the complexes is thus approximately C_{2h}, but strictly it is C_i. The chelate rings are nearly perfect planes (mean deviation ≤0.003 Å). The dihedral angles between chelate rings and aryl groups of the triazenide functions lie in the range 26–42°. The dimensions of the triazenide fragments in the two complexes differ very slightly. The N–N lengths and N–N–N angles lie within the narrow ranges 1.308(5)–1.320(7) and 103.3(4)–104.5(3)°, respectively.

The Ru–N lengths in the bivalent complex lie in the range 2.096(4)–2.116(4) Å, and the lengths in the trivalent complex are 2.058(5) and 2.066(5) Å. Thus the average length decreases by 0.04 Å upon metal oxidation. This decrease is attributed to the electrostatic effect of the greater charge on trivalent atom. This implies that the Ru–N binding is primarily σ in character.

Table 1. Bulk Magnetic Moments,[a] Molar Equivalent Conductance,[b] and Cyclic Voltammetric Reduction Potentials[c] at 298 K

compd	μ_{eff}, μ_B	Λ, Ω^{-1} cm^2 M^{-1}	$E_{1/2}$, V (ΔE_p, mV)[d]
$[Ru(HL)_2(PPh_3)_2]PF_6$	1.86	134	0.20 (80)
$[Ru(MeL)_2(PPh_3)_2]PF_6$	1.78	142	0.13 (70)
$[Ru(OMeL)_2(PPh_3)_2]PF_6$	1.82	136	0.08 (70)
$[Ru(ClL)_2(PPh_3)_2]PF_6$	1.85	140	0.37 (60)

[a] In the solid state. [b] In acetonitrile solution. [c] Conditions: solvent, dichloromethane; supporting electrolyte, TEAP (0.1 M); working electrode, platinum; reference electrode, SCE; solute concentration, ~10^{-3} M. [d] $E_{1/2} = 0.5(E_{pa} + E_{pc})$ at scan rate 50 mV s^{-1}, where E_{pa} and E_{pc} are anodic and cathodic peak potentials, respectively; $\Delta E_p = E_{pa} - E_{pc}$.

A very similar decrease in Ru–N length occurs between $Ru^{II}(NH_3)_6^{2+}$ and $Ru^{III}(NH_3)_6^{3+}$ (2.144(4) and 2.104(4) Å, respectively).[9]

In contrast, the Ru–P length increases by ~0.07 Å in going from $Ru(HL)_2(PPh_3)_2$ (2.385(2) and 2.395(2) Å) to $Ru(ClL)_2(PPh_3)_2^+$ (2.462(2) Å). This is attributed to strong back-bonding in the bivalent complex, the filled $4d_{xz,yz}$ orbitals of ruthenium transferring charge to the corresponding empty 3d orbitals of phosphorus. The effect is sufficiently powerful and goes far past offsetting the opposite electrostatic effect noted above, hence the trend reversal between Ru–N and Ru–P lengths. Back-bonding is known to be far stronger in bivalent (t_2^6) ruthenium than in the trivalent (t_2^5) metal.[10] To our knowledge, we have here the first example of a structural demonstration of back-bonding-promoted bond length order Ru^{II}–P < Ru^{III}–P in an isostructural pair of molecules. The few available results pertain to Ru–N bonds formed by π-accepting amines.[11]

The spectral, magnetic, and electrochemical properties (see below) of all the $Ru(RL)_2(PPh_3)_2$ complexes are alike, and the same is true for $Ru(RL)_2PPh_3)_2^+$. It is logical to conclude that all the complexes reported in this work are stereochemically alike, having trans configurations irrespective of the oxidation state and the R substituent.

C. Charge Transfer Spectra. Electronic spectral data for the complexes are collected in Table 4, and representative spectra are displayed in Figure 3. The trivalent species are remarkable in having an intense feature at an unusually low energy (~1200 nm). Its possible origin has been investigated in the EHMO framework of the hypothetical model complex *trans*-$Ru(H_2N_3)_2(PH_3)_2^+$ (aryl groups in **2** replaced by hydrogen) having C_{2h} symmetry.

The relevant orbitals are depicted in Figure 4. Filled ligand orbitals of a_u symmetry lie just below the metal a_g and b_g orbitals (t_{2g} in O_h). There is a hole (d^5) in the latter, and the allowed $a_u \rightarrow a_g$, b_g LMCT excitation(s) are believed to be the origin of the low-energy band. The orbital diagram applies qualitatively to the bivalent complex (d^6) also, and the allowed transition near 500 nm (Figure 3) is assigned to the a_g, $b_g \rightarrow b_u$ MLCT excitation(s).

D. Metal Redox. The bivalent (initial scan anodic) and the trivalent (initial scan cathodic) complexes give rise to the same nearly-reversible cyclic voltammetric one-electron response

(5) X = SR: (a) Pramanik, A.; Bag, N.; D.; Lahiri, G. K.; Chakravorty, A. *J. Chem. Soc., Chem. Commun.* **1991**, 139. (b) Pramanik, A.; Bag, N.; Lahiri, G. K.; Chakravorty, A. *J. Chem. Soc., Dalton Trans.* **1992**, 101. (c) Pramanik, A.; Bag, N.; Lahiri, G. K.; Chakravorty, A. *J. Chem. Soc., Dalton Trans.* **1990**, 3823.

(6) X = NR_2: (a) Pramanik, A.; Bag, N.; Chakravorty, A. *J. Chem. Soc., Dalton Trans.* **1993**, 237. (b) Menon, M.; Pramanik, A.; Bag, N.; Chakravorty, A. Unpublished results.

(7) (a) Laing, K. R.; Robinson, S. D.; Uttley, M. F. *J. Chem. Soc., Dalton Trans.* **1974**, 1205. (b) Robinson, S. D.; Uttley, M. F. *Chem. Commun.* **1971**, 1315. (c) Knoth, W. H. *Inorg. Chem.* **1973**, *12*, 38. (d) Brown, L. D.; Ibers, J. A. *Inorg. Chem.* **1976**, *15*, 2788. Brown, L. D.; Ibers, J. A. *J. Am. Chem. Soc.* **1976**, *98*, 1597.

(8) Structures of some binuclear species are known: (a) Cotton, F. A.; Falvello, L. R.; Ren, T.; Vidyasagar, K. *Inorg. Chim. Acta* **1992**, *194*, 163. (b) Cotton, F. A.; Matusz, M. *J. Am. Chem. Soc.* **1988**, *110*, 5761. (c) Cotton, F. A.; Ren, T. *Inorg. Chem.* **1991**, *30*, 3675. (d) Colson, S. F.; Robinson, S. D.; Tocher, D. A. *J. Chem. Soc., Dalton Trans.* **1990**, 629. (e) Colson, S. F.; Robinson, S. D.; Motevalli, M.; Hursthouse, M. B. *Polyhedron* **1988**, *7*, 1919.

(9) Stynes, H. C.; Ibers, J. A. *Inorg. Chem.* **1971**, *10*, 2304.

(10) (a) Taube, H. *Pure Appl. Chem.* **1979**, *51*, 901. (b) Sekine, M.; Harman, W. D.; Taube, H. *Inorg. Chem.* **1988**, *27*, 3604.

(11) (a) Richardson, D. E.; Walker, D. D.; Sutton, J. E.; Hodgson, K. O.; Taube, H. *Inorg. Chem.* **1979**, *18*, 2216. (b) Wishart, J. F.; Bino, A.; Taube, H. *Inorg. Chem.* **1986**, *25*, 3318. (c) Gress, M. E.; Creutz, C.; Quicksall, C. O. *Inorg. Chem.* **1981**, *20*, 1522. (d) Eggleston, D. S.; Goldsby, K. A.; Hodgson, D. J.; Meyer, T. J. *Inorg. Chem.* **1985**, *24*, 4573.

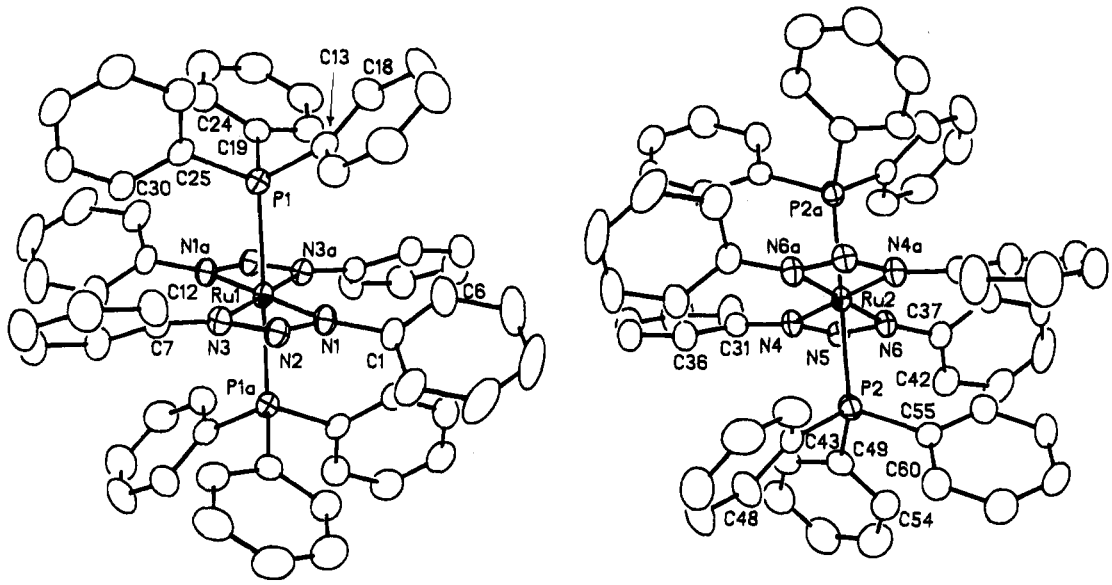

Figure 1. ORTEP plot (40% probability ellipsoids) and atom-labeling scheme for the two molecules of Ru(HL)$_2$(PPh$_3$)$_2$.

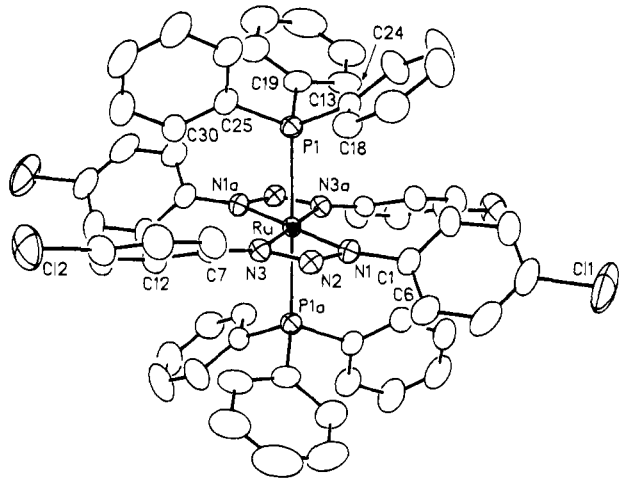

Figure 2. ORTEP plot (40% probability ellipsoids) and atom-labeling scheme for the cation of [Ru(ClL)$_2$(PPh$_3$)$_2$]PF$_6$·2CH$_2$Cl$_2$.

Table 2. Selected Bond Distances (Å) and Angles (deg) and Their Estimated Standard Deviations for Ru(HL)$_2$(PPh$_3$)$_2$

	Distances		
Ru(1)–P(1)	2.385(2)	Ru(2)–P(2)	2.395(2)
Ru(1)–N(1)	2.107(4)	Ru(2)–N(4)	2.107(4)
Ru(1)–N(3)	2.116(4)	Ru(2)–N(6)	2.096(4)
N(1)–N(2)	1.313(5)	N(4)–N(5)	1.318(6)
N(2)–N(3)	1.308(5)	N(5)–N(6)	1.317(5)
	Angles		
P(1)–Ru(1)–N(1)	92.6(1)	P(2)–Ru(2)–N(4)	92.2(1)
P(1)–Ru(1)–N(3)	89.1(1)	P(2)–Ru(2)–N(6)	88.0(1)
N(1)–Ru(1)–N(3)	58.8(1)	N(4)–Ru(2)–N(6)	59.1(1)
Ru(1)–N(1)–N(2)	98.5(2)	Ru(2)–N(4)–N(5)	98.3(2)
Ru(1)–N(3)–N(2)	98.3(2)	Ru(2)–N(6)–N(5)	98.9(3)
N(1)–N(2)–N(3)	104.5(3)	N(4)–N(5)–N(6)	103.6(4)

corresponding to the stereoretentive couple of eq 3. The two species can be quantitatively interconverted by coulometry.

$$trans\text{-}Ru(RL)_2(PPh_3)_2^{+} + e^{-} \rightleftarrows trans\text{-}Ru(RL)_2(PPh_3)_2 \quad (3)$$

The reduction potentials (Table 1) of the couple of eq 3 depend on the substituent R in the expected manner—the $E_{1/2}$ values varying linearly with the Hammett constants of R.[12] No evidence for the formation of the cis isomer supposedly having a higher $E_{1/2}$ value (see below) could be found in any of the voltammetric experiments.

Table 3. Selected Bond Distances (Å) and Angles (deg) and Their Estimated Standard Deviations for [Ru(ClL)$_2$(PPh$_3$)$_2$]PF$_6$·2CH$_2$Cl$_2$

	Distances		
Ru–P(1)	2.462(2)	N(1)–N(2)	1.315(7)
Ru–N(1)	2.058(5)	N(2)–N(3)	1.320(7)
Ru–N(2)	2.066(5)		
	Angles		
P(1)–Ru–N(1)	92.3(1)	Ru–N(1)–N(2)	98.6(3)
P(1)–Ru–N(3)	88.8(1)	Ru–N(3)–N(2)	98.0(3)
N(1)–Ru–N(3)	60.1(2)	N(1)–N(2)–N(3)	103.3(4)

E. A Contrast. The results reported above reveal that irrespective of metal valence (+2, +3) and state of aggregation (solid, solution) the triazenide complexes (**1**, **2**) occur exclusively in the trans form. In contrast, the stable geometries for **3** and **4** are respectively cis and trans. The oxidative cis → trans and

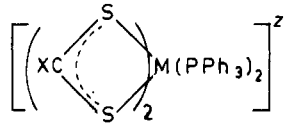

M = Ru, Os

X = OR, SR, NR$_2$

3 z = 0

4 z = +

the reductive trans → cis isomerizations are observable in solution voltammetry, $E_{1/2}$(cis) being ~0.3 V higher than $E_{1/2}$(trans).[4-6] The general features of M–S binding[4a,5a,6a] in **3** and **4** are very similar to those of Ru–N binding in Ru(RL)$_2$(PPh$_3$)$_2^z$: σ-character and the distance trends M^{III}–S < M^{II}–S, Ru^{III}–N < Ru^{II}–N. The origin of the geometrical difference between the bivalent complexes of the two families must therefore lie elsewhere.

The cis configuration has the inherent disadvantage of PPh$_3$ crowding. In the known structures[4a,5a,c,6a] of *cis*-M(XCS$_2$)$_2$(PPh$_3$)$_2$, the three carbon atoms directly bonded to one phos-

(12) (a) Mukherjee, R. N.; Rajan, O. A.; Chakravorty, A. *Inorg. Chem.* **1982**, *21*, 785. (b) Hammett, L. P. *Physical Organic Chemistry*, 2nd ed.; McGraw-Hill: New York, 1970.

Table 4. Electronic Spectral Data[a] at 298 K

compd	λ_{max}, nm[b] (ϵ, M^{-1} cm^{-1})
$Ru(HL)_2(PPh_3)_2$	510 (6300), 325 (18 600)
$Ru(MeL)_2(PPh_3)_2$	510 (8630), 330 (26 450)
$Ru(OMeL)_2(PPh_3)_2$	510 (5350), 335 (14 300)
$Cu(ClL)_2(PPh_3)_2$	510 (4150), 335 (18 050)
$[Ru(HL)_2(PPh_3)_2]PF_6$	1200 (5960), 960[b] (2700), 575[b] (1750), 455[b] (4760), 350[b] (20 200)
$[Ru(MeL)_2(PPh_3)_2]PF_6$	1200 (6600), 925[b] (1540), 575[b] (2700), 495[b] (6600), 355[b] (22 100)
$[Ru(OMeL)_2(PPh_3)_2]PF_6$	1225 (4900), 930[b] (1200), 560 (2700), 500[b] (7200), 360 (17 200)
$[Ru(ClL)_2(PPh_3)_2]PF_6$	1220 (5570), 925[b] (2200), 580[b] (1500), 500[b] (5450), 350[b] (20 300)

[a] The solvent is dichloromethane. [b] Shoulder.

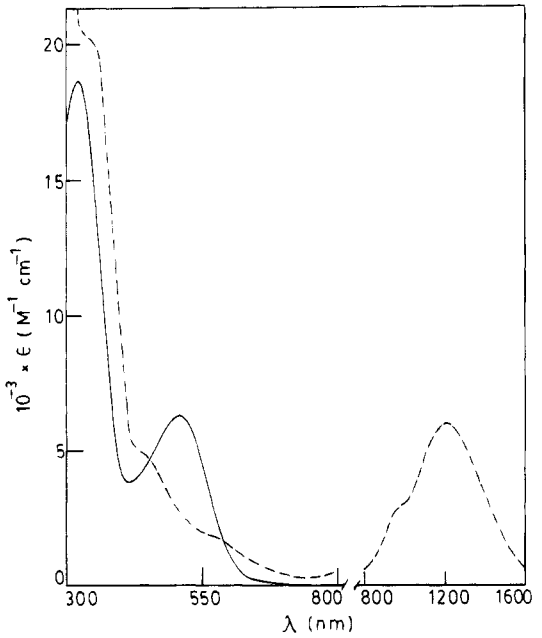

Figure 3. Electronic spectra of $Ru(HL)_2(PPh_3)_2$ (—) and $[Ru(HL)_2(PPh_3)_2]PF_6$ (- - -) in dichloromethane solution.

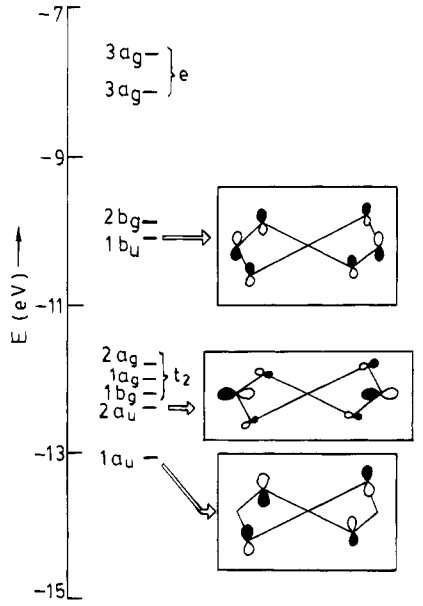

Figure 4. Selected EHMO levels of model *trans*-$Ru(H_2N_3)_2(PH_3)_2^+$.

phorus atom are invariably staggered (when viewed along the P—P axis) with respect to those simiarly bonded to the other phosphorus atom. Further the P—M—P angle is obtuse to a good degree (100—103°). In this manner, part of the PPh_3···PPh_3 repulsion is relieved[13] and M—P back-bonding, which is maximal in the cis configuration, is able to more than offset the remaining disadvantage.[4a,5a,6a] This does not happen in the triazenide system, and the cis geometry is never observed. Examination of models has indeed revealed that the triazenide phenyl rings create severe steric crowding in the cis configuration of $Ru(RL)_2(PPh_3)_2$.

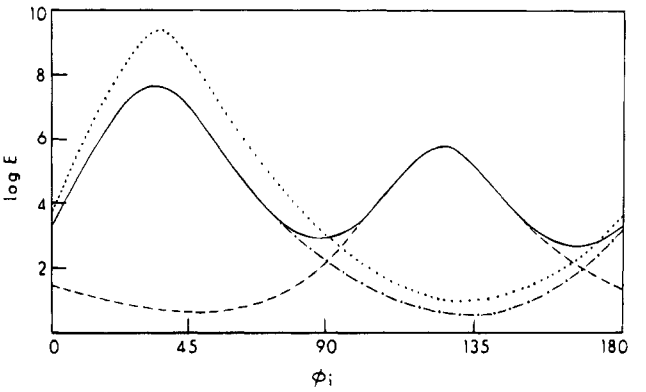

Figure 5. Angular variation of nonbonded repulsive interactions: - - -, i = 1, Ph(a)···Ph(c); — · — ·, i = 1, Ph(a)···Ph(d); —, i = 1, sum of Ph(a)···Ph(c) and Ph(a)···Ph(d); ···, i = 2, Ph(b)···Ph(c'). E is in kcal mol^{-1}, and ϕ_i is in deg.

F. Crowding in Cis Geometry. Computer models of *cis*-$Ru(HL)_2(PPh_3)_2$ of C_2 symmetry were constructed (see Experimental Section) using the available structural information[4a,5a,c,6a] on *cis*-$M(XCS_2)_2(PPh_3)_2$ as guide. A particular conformer is shown in **5**, in which the phenyl rings are labeled a—e, the

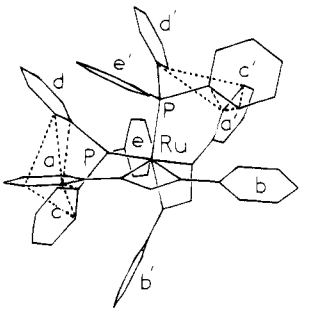

5

symmetry-equivalent rings being a'—e'. Different conformers were generated by rotating the triazenide phenyl rings Ph(a) and Ph(b) by angles ϕ_1 and ϕ_2, respectively, from the triazenide plane ($\phi_1 = \phi_2 = 0°$ at coplanarity). The major nonbonded (C···C, C···H, H···H) repulsive energies (E) arise from (Ph(a)···Ph(c), Ph(a)···Ph(d), and Ph(b)···Ph(c') interactions and their symmetry equivalents. At the broad minima ($\phi_1 = 45°$, $\phi_1 = 135°$, and $\phi_2 = 130°$, respectively) of these interactions (Figure 5) the values of E lie in the range 4—6 kcal mol^{-1}.

The main domain of crowding is Ph(a), which is cis to both the phosphine molecules. The minimum of the Ph(a)···Ph(c) interaction nearly coincides with the maximum of the Ph(a)···Ph(d) interaction and vice versa (Figure 5). The two net minima of Ph(a) repulsion correspond to E of ~700 kcal mol^{-1} ($\phi_1 = 90°$) and ~500 kcal mol^{-1} ($\phi_1 = 165°$). With symmetry-equivalent interactions added up, E will be twice as large. These are very strong repulsions which would clearly preclude the existence of the cis geometry for the $Ru(RL)_2(PPh_3)_2$ family. Structure **5**, ($\phi_1 = 165°$, $\phi_2 = 130°$) correspond to the minima of interactions for both Ph(a) and Ph(b). Even here, the Ph(a)

(13) Powell, J. *J. Chem. Soc., Chem. Commun.* **1989**, 200.

Table 5. Crystallographic Data for Ru(HL)$_2$(PPh$_3$)$_2$ and [Ru(ClL)$_2$(PPh$_3$)$_2$]PF$_6$·2CH$_2$Cl$_2$

	Ru(HL)$_2$(PPh$_3$)$_2$	[Ru(ClL)$_2$(PPh$_3$)$_2$]PF$_6$·2CH$_2$Cl$_2$
chem formula	$C_{60}H_{50}N_6P_2Ru$	$RuC_{62}N_{50}N_6Cl_8F_6P_3Ru$
fw	1018.1	1470.7
space group	$P\bar{1}$	$P\bar{1}$
a, Å	10.964(6)	11.093(6)
b, Å	11.821(7)	12.386(4)
c, Å	21.183(9)	13.757(6)
α, deg	76.52(4)	104.11(3)
β, deg	78.17(4)	103.48(4)
γ, deg	71.18(4)	110.57(3)
V, Å^3	2502(2)	1607(1)
Z	2	1
T, °C	22	22
λ, Å	0.71073	0.71073
ϱ_{calcd}, g cm^{-3}	1.351	1.520
μ, cm^{-1}	4.24	7.13
transm coeff	0.90−0.96	0.91−0.95
R^a	0.0393	0.0500
$R_w{}^b$	0.0432	0.0564
GOF^c	1.06	1.13

^{a} $R = \sum||F_o| - |F_c||/\sum|F_o|$. ^{b} $R_w = [\sum w(|F_o| - |F_c|)^2/\sum w|F_o|^2]^{1/2}$; $w^{-1} = \sigma^2|F_o| + g|F_o|^2$; g = 0.0005 for Ru(HL)$_2$(PPh$_3$)$_2$ and 0.0002 for]Ru(ClL)$_2$(PPh$_3$)$_2$]PF$_6$·2CH$_2$Cl$_2$. ^{c} The goodness of fit is defined as $[w(|F_o| - |F_c|)^2/(n_o - n_v)]^{1/2}$, where n_o and n_v denote the numbers of data and variables, respectively.

ring has a total of six C···C (distance range 2.30−2.94 Å) and seven C···H (1.72−2.46 Å) repulsive contacts with atoms of Ph(c) and Ph(d), the total repulsion amounting to $E \sim 500$ kcal mol^{-1}. For the sake of clarity, only the C···C contacts (dotted lines) have been depicted in **5**.

G. Concluding Remarks. The main findings of this work will now be summarized. The 1,3-diaryltriazene (HRL; R = H, Me, OMe, Cl) complexes Ru(RL)$_2$(PPh$_3$)$_2$ and [Ru(RL)$_2$-(PPh$_3$)$_2$]PF$_6$ of coordination type RuN$_4$P$_2$ have been synthesized and characterized. The trivalent species are unusual in having an intense near-IR LMCT band. By being uniformly trans, the present complexes represent a new situation of isomer stability among bis(phosphine) complexes of bivalent and trivalent ruthenium. Because of the invariant geometry, both states afford the same voltammogram, the $E_{1/2}$ values varying with R in the expected manner.

Metal binding of RL$^-$ is primarily σ in character (Ru^{II}−N > Ru^{III}−N), but there is substantive back-bonding within the Ru^{II}-(PPh$_3$)$_2$ motif (Ru^{II}−P < Ru^{III}−P). The bivalent cis geometry, if formed, would have had maximal back-bonding, but computer models have revealed that it is severely destabilized by crowding of certain RL$^-$ and PPh$_3$ aryl functions. In contrast, Ru^{II}-(XCS$_2$)$_2$(PPh$_3$)$_2$, having no steric interference from XCS$_2^-$, has a stable cis geometry. The trivalent species are trans in both the RL$^-$ and XCS$_2^-$ families—here back-bonding is virtually absent and the cis geometry is destabilized even by the relatively mild PPh$_3$···PPh$_3$ crowding.

Experimental Section

Materials. Commercial hydrated ruthenium trichloride obtained from Arora-Mathey, Calcutta, was converted to Ru(PPh$_3$)$_3$Cl$_2$ as reported.[14] Diaryltriazenes were synthesized by literature methods.[15] The preparation of tetraethylammonium perchlorate and the purification of solvents for electrochemical and spectroscopic work were done as before.[16] All other chemicals and solvents were of reagent grade and were used without further purification.

Physical Measurements. Electronic spectra were obtained with a Hitachi 330 spectrophotometer. Magnetic susceptibilities were measured on a PAR 155 vibrating-sample magnetometer fitted with a

Table 6. Atomic Coordinates (×10^4) and Equivalent Isotropic Displacement Coefficients (Å^2 × 10^3) for Ru(HL)$_2$(PPh$_3$)$_2$

	x	y	z	U(eq)^a		x	y	z	U(eq)^a
Ru(1)	0	0	0	27(1)	Ru(2)	0	5000	5000	29(1)
P(1)	778(1)	876(1)	686(1)	32(1)	P(1)	81(1)	2952(1)	4997(1)	34(1)
N(1)	124(4)	−1623(3)	690(2)	33(2)	N(4)	−1927(4)	5384(3)	5486(2)	36(2)
N(2)	−1034(4)	−1301(3)	1034(2)	35(2)	N(5)	−2535(4)	5693(3)	4968(2)	37(2)
N(3)	−1560(4)	−186(3)	753(2)	34(2)	N(6)	−1582(4)	5579(3)	4473(2)	37(2)
C(1)	849(5)	−2836(4)	872(2)	36(2)	C(31)	−2720(5)	5553(5)	6087(2)	38(2)
C(2)	249(6)	−3748(5)	1134(2)	51(2)	C(32)	−3927(6)	6374(6)	6139(3)	68(3)
C(3)	997(9)	−4920(5)	1301(3)	77(4)	C(33)	−4630(6)	6521(7)	6749(3)	89(4)
C(4)	2327(9)	−5203(6)	1195(3)	87(4)	C(34)	04152(6)	5849(6)	7302(3)	67(3)
C(5)	2930(7)	−4318(6)	937(3)	74(3)	C(35)	−2970(6)	5021(6)	7260(3)	62(3)
C(6)	2186(6)	−3111(5)	782(3)	54(2)	C(36)	−2248(6)	4871(5)	6651(2)	50(2)
C(7)	−2778(5)	405(4)	1077(2)	35(2)	C(37)	−1992(5)	5823(4)	3851(2)	38(2)
C(8)	−3664(5)	1293(4)	716(2)	42(2)	C(38)	−3032(5)	5475(5)	3762(3)	52(3)
C(9)	−4852(5)	1920(5)	1019(3)	53(2)	C(39)	−3397(7)	5771(6)	3137(3)	76(4)
C(10)	−5179(5)	1652(5)	1690(3)	58(3)	C(40)	−2739(8)	6370(7)	2616(3)	83(4)
C(11)	−4302(6)	750(5)	2040(3)	60(3)	C(41)	−1713(7)	6687(6)	2706(3)	67(3)
C(12)	−3108(5)	118(5)	1751(2)	46(2)	C(42)	−1332(5)	6422(5)	3314(2)	49(2)
C(13)	1696(5)	−154(4)	1332(2)	38(2)	C(43)	913(5)	1758(4)	5624(2)	38(2)
C(14)	1052(6)	−883(5)	1806(2)	48(2)	C(44)	2235(6)	1581(5)	5630(3)	59(3)
C(15)	1667(7)	−1685(6)	2305(3)	65(3)	C(45)	2885(7)	693(6)	6104(3)	71(3)
C(16)	2942(7)	−1787(6)	2348(3)	71(3)	C(46)	2244(8)	−13(6)	6560(3)	75(3)
C(17)	3581(6)	−1066(6)	1897(3)	69(3)	C(47)	970(8)	130(6)	6557(3)	74(3)
C(18)	2965(5)	−248(5)	1387(3)	51(3)	C(48)	306(6)	1013(5)	6092(3)	58(3)
C(19)	1820(5)	1839(4)	242(2)	35(2)	C(49)	−1506(5)	2668(4)	5088(2)	39(2)
C(20)	3021(5)	1338(5)	−102(3)	48(2)	C(50)	−2406(5)	2926(5)	5640(3)	48(2)
C(21)	3762(6)	2055(6)	−485(3)	61(3)	C(51)	−3632(6)	2761(5)	5723(3)	62(3)
C(22)	3320(7)	3300(6)	−527(3)	64(3)	C(52)	−3967(6)	2330(6)	5253(3)	72(3)
C(23)	2146(6)	3811(5)	−193(3)	62(3)	C(53)	−3091(6)	2056(6)	4710(3)	70(3)
C(24)	1404(5)	3096(5)	193(3)	47(2)	C(54)	−1867(5)	2215(5)	4621(3)	51(2)
C(25)	−482(5)	1916(4)	1173(2)	35(2)	C(55)	915(5)	2349(4)	4247(2)	37(2)
C(26)	−320(5)	2070(5)	1774(2)	50(2)	C(56)	1654(6)	1149(5)	4258(3)	55(3)
C(27)	−1284(6)	2891(5)	2111(3)	60(3)	C(57)	2195(6)	730(6)	3671(3)	67(3)
C(28)	−2398(6)	3559(5)	1852(3)	58(3)	C(58)	2018(6)	1477(6)	3085(3)	62(3)
C(29)	−2566(6)	3408(5)	1252(3)	55(3)	C(59)	1296(6)	2656(6)	3069(3)	58(3)
C(30)	−1609(5)	2588(4)	913(2)	41(2)	C(60)	736(5)	3108(5)	3645(3)	48(2)

^{a} Equivalent isotropic U defined as one-third of the trace of the orthogonalized U_{ij} tensor.

Walker Scientific magnet. Solution electric conductivity was measured by using a Philips PR 9500 bridge. Microanalyses (C, H, N) were done by using a Perkin-Elmer 240C elemental analyzer. Electrochemical measurements were performed on a PAR Model 370-4 electrochemistry system as described elsewhere.[4a]

Preparation of Complexes. The syntheses of complexes were achieved by using general procedures. Yields varied in the range 92–98%. Details are given for one representative complex of each type.

Bis(1,3-diphenyltriazenido)bis(triphenylphosphine)ruthenium(II), Ru(HL)$_2$(PPh$_3$)$_2$. To a suspension of Ru(PPh$_3$)$_3$Cl$_2$ (100 mg, 0.10 mmol) in warm ethanol (30 mL) was added 1,3-diphenyltriazene (50 mg, 0.25 mmol). The mixture was heated to reflux for 30 min. Upon cooling, a dark-red microcrystalline solid separated which was collected by filtration, washed thoroughly with cold ethanol, and dried in vacuo over P_4O_{10}. The yield was 103 mg (97%).

Anal. Calcd for Ru(HL)$_2$(PPh$_3$)$_2$, $RuC_{60}H_{50}N_6P_2$: C, 70.79; H, 4.92; N, 8.26. Found: C, 70.72; H, 4.90; N, 8.29. Calcd for Ru(MeL)$_2$(PPh$_3$)$_2$, $RuC_{64}H_{58}N_6P_2$: C, 71.57; H, 5.40; N, 7.83. Found: C, 71.50; H, 5.44; N, 7.81. Calcd for Ru(ClL)$_2$(PPh$_3$)$_2$, $RuC_{60}H_{46}Cl_4N_6P_2$: C, 62.34; H, 3.98; N, 7.27. Found: C, 62.30; H, 3.94; N, 7.23. Calcd for Ru(OMeL)$_2$(PPh$_3$)$_2$, $RuC_{64}H_{58}O_4N_6P_2$: C, 67.54; H, 5.10; N, 7.39. Found: C, 67.59; H, 5.12; N, 7.35.

Bis(1,3-diphenyltriazenido)bis(triphenylphosphine)ruthenium(III)Hexafluorophosphate, [Ru(HL)$_2$(PPh$_3$)$_2$]PF$_6$. To a solution of 100 mg (0.10 mmol) of Ru(HL)$_2$(PPh$_3$)$_2$ in 30 mL of dichloromethane–acetonitrile (1:1) was added 95 mg (0.15 mmol) of ceric ammonium sulfate dissolved in 20 mL of water. The mixture was stirred at room temperature for 1 h. The color of the solution changed from red to brownish red. The mixture was then filtered, and the filtrate was reduced to 10 mL under reduced pressure. A saturated aqueous solution of NH_4PF_6 (10 mL) was added to it, and the solution was kept standing overnight. The brownish red crystalline solid thus obtained was collected by filtration, washed several times with water, and dried in vacuo over P_4O_{10}. The yield was quantitative (114 mg).

Anal. Calcd for [Ru(HL)$_2$(PPh$_3$)$_2$]PF$_6$, $RuC_{60}H_{50}N_6P_3F_6$: C, 61.96; H, 4.30; N, 7.23. Found: C, 61.92; H, 4.33; 7.20. Calcd for [Ru(MeL)$_2$(PPh$_3$)$_2$]PF$_6$, $RuC_{64}H_{58}N_6P_3F_6$: C, 63.05; H, 4.76; N, 6.89. Found: C, 63.00; H, 4.79; N, 6.95. Calcd for [Ru(ClL)$_2$(PPh$_3$)$_2$]PF$_6$, $RuC_{60}H_{46}Cl_4N_6P_3F_6$: C, 55.39; H, 3.54; N, 6.46. Found: C, 55.44; H, 3.50; N, 6.40. Calcd for [Ru(OMeL)$_2$(PPh$_3$)$_2$]PF$_6$, $RuC_{64}H_{58}O_4N_6P_3F_6$: C, 59.90; H, 4.52; N, 6.55. Found: C, 59.95; H, 4.50; N, 6.60.

Recrystallization of [Ru(ClL)$_2$(PPh$_3$)$_2$]PF$_6$ from dichloromethane–hexane yielded single crystals of composition [Ru(ClL)$_2$(PPh$_3$)$_2$]PF$_6$·2CH$_2$Cl$_2$. Anal. Calcd for [Ru(ClL)$_2$(PPh$_3$)$_2$]PF$_6$·2CH$_2$Cl$_2$, $RuC_{62}H_{50}N_6Cl_8P_3F_6$: C, 50.62; H, 3.40; N, 5.72. Found: C, 50.66; H, 3.38; N, 5.75.

X-ray Structure Determination. Single crystals (0.14 × 0.18 × 0.30 mm^3 for Ru(HL)$_2$(PPh$_3$)$_2$ and 0.12 × 0.28 × 0.32 mm^3 for [Ru(ClL)$_2$(PPh$_3$)$_2$]PF$_6$·2CH$_2$Cl$_2$) grown (298 K) by slow diffusion of hexane into a dichloromethane solution were used. Cell determination, data collection, and structure solution for both the crystals were performed in the same manner unless otherwise stated.

Cell parameters were determined by least-squares fits of 30 machine-centered reflections ($2\theta = 15–30°$). Data were collected by the ω-scan technique in the range $3° \leq 2\theta \leq 50°$ on a Siemens R3m/V four-circle diffractometer with graphite-monochromated Mo Kα radiation ($\lambda = 0.71073$ Å). Two check reflections measured after every 98 reflections showed no significant intensity reduction. All data were corrected for Lorentz, polarization, and absorption.[17] Of the 9361 (Ru(HL)$_2$(PPh$_3$)$_2$) and 6043 ([Ru(ClL)$_2$(PPh$_3$)$_2$]PF$_6$·2CH$_2$Cl$_2$) reflections collected, 8853 and 5700 were unique of which 4989 and 3725 were respectively taken as observed ($I > 3\sigma(I)$) for structure solution and refinement. There were no systematic absences and the structures were successfully solved in the space group $P\bar{1}$.

The metal positions were located from Patterson maps, and the rest of the non-hydrogen atoms emerged from successive Fourier syntheses. The structures were then refined by full-matrix least-squares procedures. All non-hydrogen atoms were refined anisotropically, and hydrogen atoms were added at calculated positions with fixed $U = 0.08$ Å^2 in the final cycle of refinement. The highest residuals were 0.31 and 0.83 e Å^{-3}, respectively, for Ru(HL)$_2$(PPh$_3$)$_2$ and [Ru(ClL)$_2$(PPh$_3$)$_2$]PF$_6$·2CH$_2$Cl$_2$. All calculations were done on a MicroVAX II computer using the SHELXTL-Plus program package.[18] Significant crystal data are listed in Table 5, and atomic coordinates and isotropic thermal parameters are collected in Tables 6 and 7.

Table 7. Atomic Coordinates (×10^4) and Equivalent Isotropic Displacement Coefficients (Å^2 × 10^3) for [Ru(ClL)$_2$(PPh$_3$)$_2$]PF$_6$·2CH$_2$Cl$_2$

	x	*y*	*z*	*U*(eq)[a]
Ru	0	0	0	27(1)
P(1)	−542(1)	−1961(1)	−1381(1)	36(1)
P(2)	0	0	5000	69(1)
Cl(1)	−4890(3)	1477(2)	−3911(2)	127(1)
Cl(2)	−4277(2)	−4471(2)	2223(2)	89(1)
N(1)	−1817(4)	19(4)	−769(3)	35(2)
N(2)	−2602(4)	−629(4)	−341(3)	36(2)
N(3)	−1754(4)	−893(4)	3013)	34(2)
F(1)	−1425(7)	−293(8)	4243(5)	157(5)
F(2)	485(6)	−164(5)	4008(4)	119(3)
F(3)	−504(8)	−1413(5)	4765(5)	140(4)
C(1)	−2519(5)	427(5)	−1501(4)	41(2)
C(2)	−2261(6)	366(5)	−2449(5)	50(3)
C(3)	−2984(8)	693(6)	−3198(5)	64(3)
C(4)	−3939(8)	1087(6)	−2971(6)	70(4)
C(5)	−4184(7)	1172(6)	−2030(7)	66(3)
C(6)	−3466(6)	843(5)	−1288(5)	53(3)
C(7)	−2396(5)	−1734(5)	761(4)	36(2)
C(8)	−3775(6)	−2554(6)	290(5)	51(3)
C(9)	−4365(7)	−3389(6)	742(5)	58(3)
C(10)	−3562(7)	−3401(5)	1661(5)	54(3)
C(11)	−2203(7)	−2597(6)	2141(5)	57(3)
C(12)	−1618(6)	−1765(5)	1686(5)	47(3)
C(13)	−1984(6)	−2448(5)	−2608(4)	40(2)
C(14)	−1854(7)	−2522(6)	−3598(5)	61(3)
C(15)	−3015(9)	−2916(8)	−4498(6)	85(4)
C(16)	−4269(8)	−3276(7)	−4418(6)	73(4)
C(17)	−4443(7)	−3227(6)	−3446(6)	65(3)
C(18)	−3295(6)	−2805(5)	−2544(5)	49(3)
C(19)	915(6)	−1967(5)	−1783(5)	47(3)
C(20)	1535(7)	−2712(7)	−1550(6)	65(3)
C(21)	2702(9)	−2628(9)	−1816(8)	89(5)
C(22)	3204(9)	−1859(9)	−2313(8)	97(5)
C(23)	2581(8)	−1142(7)	−2579(7)	78(4)
C(24)	1453(7)	−1179(5)	−2307(5)	58(3)
C(25)	−1060(6)	−3299(5)	−981(5)	43(3)
C(26)	−1903(7)	−4465(5)	−1758(6)	65(3)
C(27)	−2248(8)	−5479(6)	−1465(7)	80(4)
C(28)	−1867(8)	−5363(6)	−423(7)	72(4)
C(29)	−1029(8)	−4220(7)	357(6)	66(4)
C(30)	−625(6)	−3198(5)	62(5)	47(3)
C(31)	861	6679	4667	230(14)
Cl(3)	−271(15)	5848(9)	3528(7)	470(12)
Cl(4)	2070(11)	6181(19)	4738(7)	541(20)

[a] Equivalent isotropic *U* defined as one-third of the trace of the orthogonalized U_{ij} tensor.

Molecular Orbital Calculations. Extended Huckel calculations were performed on an IBM PC AT using the ICON software package originally developed by Hoffmann.[19] The atomic parameters and H_{ii} values for N, P, H, and Ru were taken from the literature.[20] The orthogonal coordinate system chosen for calculation is defined in Figure 4. The averaged experimental bond distances and angles were used in our calculations. The N-H distance was taken as 0.90 Å.

Cis Models with Repulsion Energies. Models of *cis*-Ru(HL)$_2$(PPh$_3$)$_2$ were generated with the help of the interactive molecular

(14) Stephenson, T. A.; Wilkinson, G. J. *Inorg. Nucl. Chem.* **1966**, *28*, 945.
(15) Hartman, W. W.; Dickey, J. B. *Org. Synth.* **1943**, *2*, 163.
(16) (a) Chakravarty, A. R.; Chakravorty, A. *J. Chem. Soc., Dalton Trans.* **1982**, 615. (b) Mahapatra, A. K.; Datta, S.; Goswami, S.; Mukherjee, M.; Mukherjee, A. K.; Chakravorty, A. *Inorg. Chem.* **1986**, *25*, 1715.
(17) North, A. C. T.; Philips, D. C.; Mathews, F. S. *Acta Crystallogr., Sect. A* **1968**, *A24*, 351.
(18) Sheldrick, G. M. *SHELXTL* Plus, *Structure Determination Software Programs*; Siemens Analytical X-ray Instruments Inc.: Madison, WI, 1990.

graphics program XP compatible with SHELXTL-Plus.[18] The four known structures[4a,5a,c,6a] of *cis*-M(XCS$_2$)$_2$(PPh$_3$)$_2$ have the following common features: (a) P−M−P angle, 100−103°; (b) the two PC$_3$ fragments, staggered when viewed down P−P axis; (c) molecular symmetry, C_2 or near-C_2. These features were incorporated into the model (P−M−P, 100°; staggering as above; molecular symmetry, C_2). The relative orientation of the phosphine phenyl rings are not identical in the four known structures of *cis*-M(XCS$_2$)$_2$(PPh$_3$)$_2$. The results described conform to the orientation observed in *cis*-Os(EtSVS$_2$)$_2$-(PPh$_3$)$_2$.[5a] We have however checked that other orientations lead to very similar repulsion profiles. Model building was completed by replacing the MS$_2$C chelate ring by the RuN$_3$ ring with distances and angles set at Ru−N = 2.10 Å, N−N = 1.32 Å, N−Ru−N = 60°, and N−N−N = 105°. These values conform to those found in *trans*-Ru-(HL)$_2$(PPh$_3$)$_2$. The triazenide phenyl rings were given the following length and angle parameters: C−C, 1.40 Å; C−C−C, 120°. The C−N length was set at 1.35 Å. The angles ϕ_1 and ϕ_2 defined in the text were varied in steps of 15° in the range 0−180°.

Nonbonded interaction energies were calculated with the help of eq 4 where x represents the distance (in Å) between the ith and jth atoms

$$E = -A_{ij}/x^6 + B_{ij}/x^{12} \quad (4)$$

and A_{ij} and B_{ij} are constants for attractive and repulsive interactions, respectively, between atoms i and j. Values of A_{ij} and B_{ij} for C···C, C···H, and H···H interactions were calculated from the available values of the closely related parameters.[21]

Acknowledgment. We are thankful to the Department of Science and Technology and the Council of Scientific and Industrial Research for financial support. Affiliation to the Jawaharlal Nehru Centre for Advanced Scientific Research is gratefully acknowledged.

Supplementary Material Available: For Ru(HL)$_2$(PPh$_3$)$_2$ and [Ru-(ClL)$_2$(PPh$_3$)$_2$]PF$_6$·2CH$_2$Cl$_2$, tables of complete bond distances (Tables S1 and S5) and angles (Tables S2 and S6), anisotropic thermal parameters (Tables S3 and S7), and hydrogen atom positional parameters (Tables S4 and S8) (10 pages). Ordering information is given on any current masthead page.

IC941017J

(19) (a) Hoffmann, R. *J. Chem. Phys.* **1963**, *39*, 1397. (b) Ammeter, J. H.; Burgi, H.-B.; Thebeault, J. C.; Hoffmann, R. *J. Am. Chem. Soc.* **1978**, *100*, 3686.

(20) (a) Tatsumi, K.; Hoffmann, R. *J. Am. Chem. Soc.* **1981**, *103*, 3328. (b) Hoffman, D. M.; Hoffmann, R.; Fisel, C. R. *J. Am. Chem. Soc.* **1982**, *104*, 3858. (c) Siedle, A. R.; Newmark, R. A.; Pignolet, L. H.; Wang, D. X.; Albright, T. A. *Organometallics* **1986**, *5*, 38.

(21) Rappé, A. K.; Casewit, C. J.; Colwell, K. S.; Goddard, W. A., III; Skiff, W. M. *J. Am. Chem. Soc.* **1992**, *114*, 10024.